Published in final edited form as:
*Mol Cancer Ther*. 2015 February ; 14(2): 513–522. doi:10.1158/1535-7163.MCT-14-0208.

# Sunitinib dose-escalation overcomes transient resistance in clear cell renal cell carcinoma and is associated with epigenetic modifications

**Remi Adelaiye**[1,2], **Eric Ciamporcero**[1,3], **Kiersten Marie Miles**[1], **Paula Sotomayor**[1,4], **Jonathan Bard**[5], **Maria Tsompana**[5], **Dylan Conroy**[1], **Li Shen**[1], **Swathi Ramakrishnan**[1,2], **Sheng-Yu Ku**[1,2], **Ashley Orillion**[4], **Joshua Prey**[6], **Gerald Fetterly**[6], **Michael Buck**[5], **Sreenivasulu Chintala**[1,7], **Georg A. Bjarnason**[8,*], and **Roberto Pili**[1,2,*]

[1]Genitourinary Program, Roswell Park Cancer Institute, Buffalo NY, USA

[2]Department of Cancer Pathology and Prevention, Roswell Park Cancer Institute Division, University at Buffalo, Buffalo NY, USA

[3]Department of Medicine and Experimental Oncology, University of Turin, Turin Italy

[4]Department of Molecular and Cellular Biology, Roswell Park Cancer Institute, Buffalo NY, USA

[5]Center of Excellence in Bioinformatics and Life Sciences, University at Buffalo, Buffalo NY, USA

[6]Pharmacokinetics and Pharmacodynamics Core Facility, Roswell Park Cancer Institute, Buffalo NY, USA

[7]Department of Pharmacology and Therapeutics, Roswell Park Cancer Institute, Buffalo NY, USA

[8] Sunnybrook Odette Cancer Center, University of Toronto, Toronto ON, Canada

## Abstract

Sunitinib is considered a first-line therapeutic option for patients with advanced clear cell renal cell carcinoma (ccRCC). Despite sunitinib clinical efficacy, eventually patients develop drug resistance and disease progression. Herein, we tested the hypothesis whether initial sunitinib resistance may be transient and could be overcome by dose increase. In selected patients initially treated with 50 mg sunitinib and presenting with minimal toxicities, sunitinib dose was escalated to 62.5 mg and/or 75 mg at the time of tumor progression. Mice bearing two different patient-derived ccRCC xenografts (PDXs) were treated 5 days/week with a dose-escalation schema (40-60-80 mg/kg sunitinib). Tumor tissues were collected prior to dose increments for immunohistochemistry analyses and drug levels. Selected intra-patient sunitinib dose escalation was safe and several patients had added progression free survival. In parallel, our preclinical results showed that PDXs, although initially responsive to sunitinib at 40 mg/kg, eventually developed resistance. When the dose was incrementally increased, again we observed tumor response to sunitinib. A resistant phenotype was associated with transient increase of tumor vasculature despite intratumor sunitinib accumulation at higher dose. In addition, we observed

Reprints should be sent to: Georg Bjarnason MD, Odette cancer Centre, 2075 Bayview Ave, Toronto ON M4N 3M5 georg.bjarnason@utoronto.ca. Roberto Pili MD, Roswell Park Cancer Institute, Elm&Carlton Streets, Buffalo, NY 14263 Roberto.Pili@RoswellPark.org.

associated changes in the expression of the methyltransferase EZH2 and histone marks at the time of resistance. Furthermore, specific EZH2 inhibition resulted in increased *in vitro* anti-tumor effect of sunitinib. Overall, our results suggest that initial sunitinib-induced resistance may be overcome, in part, by increasing the dose, and highlight the potential role of epigenetic changes associated with sunitinib resistance that can represent new targets for therapeutic intervention.

**Keywords**

sunitinib; drug resistance; clear cell renal cell carcinoma; epigenetic modifications

## INTRODUCTION

Renal cell carcinomas (RCC) are responsible for ~85% of all primary renal neoplasms (1). It is ranked among the top 10 most common cancers in the United States with an estimated incidence of 65,150 and 13,680 deaths expected to have occurred in 2013 (1,2). Among the histological types of RCC, clear cell renal cell carcinoma (ccRCC) is the most common type arising from the proximal tubules, and accounting for 75 to 85% of RCC tumors. This histological type of RCC often presents with deletion of chromosome 3p that harbors the *Von Hippel-Landau* (*VHL*) gene (2,3).

Recent advances in the management of recurrent RCC have established agents targeting vascular endothelial growth factor (VEGF), such as sunitinib, as the standard initial therapeutic option (4). Sunitinib, a multi-targeted tyrosine kinase inhibitor (TKI), is a FDA approved anti-angiogenic agent that primarily targets vascular endothelial growth factor receptors (VEGFRs) and platelet-derived growth factor receptors (PDGFRs) (5). In a randomized phase III clinical study, sunitinib was shown to prolong progression-free survival in patients with metastatic RCC (4). Despite its clinical efficacy, the majority of patients, who initially responded to sunitinib, eventually develop resistance and progress. Several potential mechanisms responsible for acquired resistance to anti-VEGF drugs have been proposed such as the continuous activation of the VEGF axis via upstream or downstream effectors (6-9). Other factors that may contribute to sunitinib resistance include activation of VEGF independent pathways such as bFGF, c-met, IL-8 or other angiogenic cytokines (10), altered pharmacokinetics, drug sequestration (11), or epithelial to mesenchymal transition (12).

Epigenetic modifications of histone protein in the chromatin have been shown to play an important role regulating the fidelity of gene transcription patterns in cells by the catalytic activity of histone deacetyalses and methyltransferase (13). The enhancer of zeste homologue 2 (EZH2), a catalytic subunit of the polycomb repressive complex 2 (PRC2), is a histone methyltransferase that catalyzes the methylation of lysine 27 on histone 3 and tri-methylation of lysine 27 on histone 3 (H3K27me3) leads to the repression of gene expression (14). Overexpression of EZH2 has been implicated in a variety of cancer types. In addition, EZH2 has been shown to contribute to tumor angiogenesis by inactivating anti-angiogenic factors via methylation at their promoter region (15). Posttranslational

modifications on the tri- and di-methylated H3K4 have been associated with the regulation of angiogenesis and migration *via* the CCL14 chemokine pathway (16).

Herein, we report the preclinical and clinical effect of introducing a sunitinib dose escalation regime as a therapeutic strategy to overcome initial drug induced resistance in ccRCC. We also show that drug resistance may be associated with epigenetic changes such as the overexpression of methyltransferase EZH2 and modulation of histone marks.

## MATERIALS AND METHODS

### Cell lines and establishment of sunitinib resistant cell line

The 786-0 renal cell carcinoma cell lines were obtained from American type culture collection (ATCC, Manassas, VA). Cells are routinely (every 6 months) tested in the lab for mycoplasma contamination using mycoplasma detection kit in accordance to manufacturer's instructions (Life Technologies, Grand Island, NY). No authentication of human genotype was done by the authors. Cells were maintained in 5% $CO_2$ at 37°C in RPMI media supplemented with 10% Fetal Bovine Serum (FBS) and 0.1% penicillin-Streptomycin. Sunitinib resistant cell lines 786-0R, were established by exposing 786-0 cells to an initial dose of sunitinib (2uM) and gradually increasing concentrations up to 5uM. Resistant cell lines, 786-0R were then continuously exposed to 5uM of sunitinib.

### EZH2 short hairpin RNA (shRNA) stable transfection

We used four unique 29mer shRNA constructs, as well as a scrambled negative control non-effective shRNA packaged in a lentiviral green fluorescent protein (GFP) vector which were purchased form Origene Technologies, Inc. (Rockville, MD). 786-0 cells which have considerably higher expression of EZH2 and less responsive to sunitinib (IC50 = 5uM) were plated for 24 hours. At approximately 60% confluence, cells were transfected using polybrene (Sigma-Aldrich, St. Louis, MO) according to the manufacturer's instructions. Stable clones were selected with puromycin (5ug/ml) starting at 48 hours after transfection. All infected cells were assayed by Western blot analysis and quantitative real time PCR to determine the efficiency of shEZH2 knockdown. Stable transfected cells were propagated and maintained in media containing puromycin (5ug/mL).

### Xenograft Models

RP-R-01 and RP-R-02 are patient derived ccRCC models. RP-R-01 was established from a skin metastasis in a patient with sporadic ccRCC who initially responded to sunitinib treatment but developed drug resistance. RP-R-01 is characterized by the deletion of the VHL gene (12). RP-R-02 was developed from a skin metastasis in a patient with hereditary ccRCC (VHL syndrome) who was treatment naíve. RP-R-01 and RP-R-02 ccRCC models had undergone several passages *in vivo* and still maintain the clear cell morphology (Fig. 1A). All *in vivo* experiments were approved and performed in strict accordance with the guidelines of the Institutional Animal care and use committee (IACUC) at Roswell Park Cancer Institute. Six weeks old homozygous Icr Severe Combined Immune-deficient (SCID) female mice were housed in a sterile, pathogen-free facility and maintained in a temperature controlled room under a 12 hour light/dark schedule with water and food ad libitum. RP-

R-01 and RP-R-02 viable tumors were selected and dissected into ~1mm$^2$ tumor pieces and implanted subcutaneously into mice. All mice were operated under sedation with oxygen, isoflurane and buprenorphine. When tumors were established, mice were randomly grouped and placed in either control group or treatment group (n=20).

### Sunitinib treatment and dose escalation schedule

Sunitinib was provided by Pfizer pharmaceuticals. Mice bearing either RP-R-01 or RP-R-02 tumors were randomly grouped into control and treatment groups. Mice in treatment groups were treated with a starting dose of 40 mg/kg (sunitinib free base) 5 days on, 2 days off by oral gavage. Treatment dose was increased to 60mg/kg when tumors were observed to be resistant to the initial dose and then subsequently to 80mg/kg. Tumors were defined to be sensitive when either stable growth or regression was observed following start of treatment. Tumors were defined resistant when a ≥50% increase in tumor growth from baseline was observed on treatment. Tumor volumes were measured once a week by caliper measurement according to the formula: tumor volume (mm$^3$) = longest length × shortest length$^2$ X 0.5. Body weights were assessed once a week using a weighing scale and recorded in grams. Endpoint tumor weights were assessed using a weigh scale and recorded in grams.

### Blood and tissue collection

Tissue and blood were collected under aseptic conditions. 200μl of blood was collected by submandibular bleeds prior to treatment or when tumors were responsive to treatment and 1ml of blood by cardiac bleeds (terminal) when tumors were non responsive to treatment, prior to dose escalation. Serum and plasma were separated and aliquots were stored at −80°C for further analysis. Tumor tissues were excised, weighed and cut into sections. Sections were snap-frozen and stored in −80°C, fixed in 10% buffered formalin or zinc for histopathology.

### Clinical ccRCC Patients

Sequential ccRCC patients seen at either the Sunnybrook Odette Cancer Centre and Roswell Park Cancer Institute who presented with progression at the standard sunitinib dose and schedule (daily 50 mg, 4 weeks on/2 weeks off) on imaging and with < grade-2 toxicity were offered sunitinib dose escalation (62.5 mg and 75 mg, 2 weeks on, 1 week off). The number presented is the total of patients that were offered before an ongoing prospective study started, and represents ~10% of patients treated with sunitinib. Grade-2 toxicities such mucositis, diarrhea, hematological, and hand-foot syndrome prevented patients to be considered for sunitinib dose escalation. Hypertension (controlled), hypothyroidism and skin discoloration were not considered significant toxicities. Patients with no overt toxicities were treated to some type of grade-2 toxicity (mucositis, diarrhea, hematological, hand foot syndrome). Patients were routinely monitored for side effects and underwent imaging for tumor response assessment at standard time intervals. Every patient was informed about the rationale behind the dose-escalation and the discussion was documented in the physician note. Patients understood that they were individually dose reduced based on toxicity and that we were individually dose escalating based on toxicity. Ultimately, all the patients that progressed on the escalated dose of sunitinb received 2$^{nd}$ line therapies as well.

### *In vitro* assays

786-0 and 786-0R cells were seeded in 24 wells plates (Santa Cruz biotechnology, Dallas, Texas) and allowed to attach for 24 hours. Afterwards, cells were treated with increases concentrations of sunitinib (LC laboratories, Woburn, MA), the EZH2 inhibitor GSK126 (Cayman chemical company, Ann Arbor, Michigan) or combination of both sunitinib and GSK126 using combination index values (Calcusyn software). Cell were fixed and stained with crystal violet (Sigma Aldrich, St. Louis, MO) after 48h of treatment. Afterwards, stained cells were washed with $ddH_2O$ to remove excess dye, air-dried and dissolved in methanol. Cells viability was quantitated by absorbance using a spectrometer at 570nm (xMarks Spectrometer, Bio-Rad). 786-0shRNA (scramble) and 786-0shEZH2 were seeded in 24 well plates and 24 hours later, cells were treated with 2μM, 4μM, 6μM and 8μM of sunitinib. After 48 hours of treatment, cells were fixed, stained and read using spectrometer.

### Measurement of sunitinib concentrations by LC/MS/MS methods

For the sunitinib pharmacokinetic studies, at the time of sensitivity to 40mg/kg dose, blood and tumor samples were collected 24 hours post treatment (7 days post treatment start date) in the RP-R-01 model. At the time of resistance to 40mg/kg dose (day 74 on treatment), the second tumor and blood samples via terminal bleed from the same group of mice were collected. The last collection occurred on day 92 and day 153 at the time of response to 60 mg/kg dose and resistance, respectively. An LC/MS/MS method was used to determine sunitinib and its metabolite Su-12662 plasma concentrations. Calibrators and QC samples were prepared in normal human plasma and extracted in duplicate along with patient samples. Calibrators ranged from 1-1000ng/ml for sunitinib and 0.5-1000ng/ml for Su-12662. QC samples were prepared at 3, 75, and 750ng/ml. Samples were extracted by protein precipitation using a TomTec Quarda 4 robotic system. Briefly, 50μl of sample, standard, or QC was added to a 96well plate, 150μl of ACN containing the internal standard D, L, propranolol was added to each well and the plate vortexed and centrifuged, 100μl of supernatant was then added to a clean 1ml plate containing 100μl of 10mM ammonium formate pH 5.0, plate was then vortexed and centrifuged briefly and 10μl were injected. Analysis was carried out using a Thermo Scientific TSQ quantum Ultra triple quad mass spectrometer in positive APCI mode. The mass transitions monitored are as follows: Sunitinib 399.17/282.91; Su-12662 371.17/282.913; and D, L, Propranolol (IS) 260.17/116.06. Chromatographic separation was carried out using a Luna CN 5μm 50X2.0mm column with a mobile phase consisting of 50:50 10mM ammonium formate pH 5.0: acetonitrile at a flow rate of 950μl/min. Column temperature was maintained at 30°C while samples were maintained at 4°C. Unknown concentrations were calculated based on the weighted $1/x^2$ linear regression of the calibrators. Tissue extraction consisted of adding 280μl of 20%MeOH diluent to tissue sample with 4 3mm stainless steel beads and processed using a bullet blender.

### Histological and Immunohistochemistry analysis

Tissue specimens were fixed for 24-hr, paraffin embedded and sectioned (5μm). Sections were de-paraffinized and rehydrated through graded alcohol washes. Antigen unmasking was achieved by boiling slides in either sodium citrate buffer (pH=6.0) or EDTA. H&E

staining was performed by the standard methods. For immunohistochemistry staining (IHC), sections were further incubated in hydrogen peroxide to reduce endogenous activity. To examine the expressions of our proteins of interests, tissue section were blocked with 2.5% horse serum (Vector Laboratories) and incubated overnight in primary antibodies against Ki67 (1:500, Thermo Fisher) and CD31 (1:100, Dianova), EZH2 (1:100, Cell Signaling), H3K27me3 (1:200, Cell Signaling) , H3K4me2 (1:1500, Cell Signaling), H3K4me3 (1:800, Cell Signaling) and H3K9me2 (1:200, Cell Signaling). Following primary incubation, tissue sections were incubated in horseradish-conjugated anti-rabbit or anti-rat antibody according to manufacturer's protocol (Vector Laboratories) followed by enzymatic development in diaminobenzidine (DAB) and counter stained in hematoxyline. Section were dehydrated and mounted with cytoseal 60 (Thermo Scientific). Respective isotype negative controls were used for evaluation of specific staining. Stained sections were analyzed either under bright field (IHC) using the Zeiss Axio microscope. The number of positive cells was determined in a blinded fashion by analyzing four random 20x fields per tissue and quantified using Image J software.

## Western blot analysis

Control and treated 786-0 cells were lysed in RIPA buffer (Sigma-Aldrich) supplemented with Protease and Phosphatase Inhibitor Cocktails (Pierce). Protein concentrations were determined by Bradford assay (Bio-Rad). Samples containing 50μg of protein underwent electrophoresis on 12% SDS polyacrylamide gels and transferred onto nitrocellulose membranes. Proteins of interests were detected using the following primary antibodies; EZH2 (1:1000, Cell Signaling), E-cadherin (1:1000, Cell signaling) E2F-1 (1:1000, Cell Signaling) and β-actin (Santa Cruz biotechnology). After incubation with HRP-conjugated secondary antibodies (Bio-Rad), membranes were exposed chemiluminesce according to manufacturer's instructions (Thermo Fisher Scientific) and captured on film. Quantitative measurements of Western analysis were performed using ImageJ and GraphPad software (Prism 6).

## RNA isolation and quantitative RT-PCR

Total RNA was isolated using the Trizol reagent (Life Technologies) according to the manufacturer's instructions and measured using the nano-drop (purity ≥ 1.89). Quantitative RT-PCR was performed utilizing EZH2, E-cadherin and GAPDH human-specific primers (IDT Technologies). The denaturation step was carried out at 95°C for 10 secs, annealing step was carried out at 58°C for 30 seconds and extension step at 72°C for 1 min using the CFX connect real-time system (Bio-Rad). CFX software was used to identify cycle threshold (Ct) values and generate gene expression curves, all data were normalized to GAPDH expression.

## Exome sequencing

**Sample preparation—**DNA libraries for the samples were prepared using the TruSeq DNA Sample v2 preparation kit (Illumina, Inc.) as per manufacturer's instructions. 1ug of each DNA sample was fragmented using Covaris shearing to a size range of 300 – 400bp. Following end repair and 3' adenylation, indexing adapters were ligated to the fragment

ends. Following purification, the fragmented DNA was PCR amplified for 5 cycles, purified and validated for appropriate size on a 2100 Bioanalyzer High Sensitivity DNA chip (Agilent Technologies, Inc.). Each DNA library was quantitated using quantitative PCR (KAPA Biosystems) prior to exome capture.

**TruSeq exome capture—**500ng of each TruSeq DNA library was pooled (6-plex) and enriched for exome sequences using the TruSeq Exome Enrichment Kit (Illumina, Inc.) as per manufacturer's instructions. Following two rounds of hybridization to the capture baits, the enriched library was PCR amplified for 10 cycles, AMPure XP bead purified, and validated for appropriate size on a 2100 Bioanalyzer High Sensitivity DNA chip (Agilent Technologies, Inc.). The enriched library was quantitated using quantitative PCR (KAPA Biosystems) and normalized to 8pM.

### Statistical analysis

Data analyses are expressed as the mean ± standard error of mean (SEM). Statistical significance, where appropriate was evaluated using a two tailed student *t* test when comparing two groups or by one-way analysis of variance (ANOVA) using the student-Newman keuls post-test for multiple comparison. A p value $< 0.05$ was considered to be significant; *p $<0.05$, **p $< 0.01$, ***p $<0.001$, ns= not significant. Statistical analyses were performed by using GraphPad Prism Software (La Jolla, CA).

## RESULTS

### Sunitinib dose-escalation overcomes drug-induced resistance in RP-R-01 and RP-R-02 ccRCC PDX models

To evaluate the effect a sunitinib dose escalation regime and overcome transient drug resistance *in vivo*, we utilized the RP-R-01 and RP-R-02 PDX models. These VHL negative models maintain the original clear cell morphology, human Alu sequence and contain common ccRCC gene mutations including *PBRM1*, *SETD2* and *KDM6A* (Fig. 1 A-B and Supplementary Fig. 1). In a first set of experiments we implanted RP-R-01 tumors under the skin of mice (Supplementary Fig. 2A). When tumors reached a palpable size, we separated mice into 2 groups; Control group and sunitinib treatment group. Then, we started sunitinib at the dose of 30 mg/kg and we monitored tumor growth. When the tumors became resistant we excised them and re-implanted in mice. As they reached a palpable size we increased the sunitinib dose to 45 mg/kg. We repeated the same schema with 60 mg/kg dose. Our results showed a dose dependent effect of sunitinib and a transient drug acquired resistance. In view of these preliminary data, we decided to conduct an intra-mouse dose escalation experiment in both RP-R-R01 and RP-R-02 models. In this new set of experiments, as tumors became resistant they were not excised and continued to be treated at higher doses. Our data show that at the starting dose of 40 mg/kg, tumors were responsive to sunitinib in both RP-R-01 and RP-R-02 models as suggested by the regression in tumor size (Fig.1C-D). However, after 4 weeks of treatment, RP-R-01 tumors began to grow despite sunitinib treatment. Although RP-R-02 showed significant response to sunitinib treatment, these PDX tumors eventually became resistant to treatment at day 84. Then, we increased the dose from 40 mg/kg to 60 mg/kg and observed again a decrease in tumor growth. However, following a

period of stabilization tumors began to grow. Finally, as we increased the dose to 80 mg/kg and, we noticed again inhibition in tumor growth. Mice under sunitinib dose escalation regime showed no signs of drug toxicity such as loss of body weight (Supplementary Fig. 3A), lethargy, abnormal behavior or loose stool, although we noticed yellowing of paws and furs. Histopathology assessment of the liver tissues from mice on dose escalation studies indicated no vascular changes, hematoma formation or necrosis (Supplementary Fig. 3B). In a separate set of experiments, we started treating both RP-R-R01 and RP-R-R02 directly at 80 mg/kg sunitinib dose. As shown in Fig. 1E-F, RP-R-01 tumors initially regressed but eventually became resistant to sunitinib within 4 months. In contrast, high dose of sunitinib induced a prolonged tumor response in the RP-R-02 model, suggesting again the dose-dependent effect of sunitinib on tumor growth.

### Micro-vessel density changes, proliferation status with initial response and subsequent resistance to sunitinib

To determine whether the transient response and resistance to sunitinib in the PDX model RP-R-01 was associated with reversible biological effects, we assessed micro vessel density and proliferation activity by immunohistochemistry analyses of CD31 and Ki67 staining, respectively. We observed a decrease in tumor vasculature with response to sunitinib treatment, which was expected. However, sunitinib resistant tumors became hyper-vascularized again (Fig. 2A). Ki67 staining also showed increased proliferation with resistance to sunitinib treatment. Similar patterns were observed in the RP-R-02 model (Fig. 2B).

### Intra-tumor and plasma concentrations of sunitinib

To determine whether the transient sunitinib resistance was due to reduction of drug levels we assessed the concentration of sunitinib in the tumor and in the circulation at the time of response and when tumors became resistant. We utilized a state-of-the-art, quantum ultra-triple mass spectrometer in APCI positive mode. RP-R-01 tumor tissues and plasma samples were measured for sunitinib concentration and its metabolite Su-12662. Supplementary Fig. 4A showed that there was a reduction in the plasma concentrations of sunitinib and its metabolite in the tumors when they became resistant at 40 mg/kg dose. Similar reduction, though not statistically significant, was observed in the tumors resistant at 60 mg/kg dose. However, in contrast to the plasma concentrations, we observed increased intratumoral concentrations of sunitinib at higher doses, though not statistically significant (Supplementary Fig. 4B). As previously reported, intra-tumor sunitinib concentrations were >10 fold higher than those in the plasma (11, 12).

### Resistance to sunitinib is associated with epigenetic changes in ccRCC PDX models and a ccRCC patient tissue sample

Previous studies have shown that epigenetic changes including differential expression of the histone methyltransferase EZH2 may be associated with drug resistance (17-18). A survey of over 400 ccRCC tumors from the TCGA data portal identified several changes in the methylation status of the lysine tails of histone 3 and the associated mutated genes with progression of disease to advance staged (19). Based on these evidences, we were interested in assessing the expression levels of EZH2 and the methylation status of histone marks

(H3K27me3, H3K4me2, H3K4me3 and H3K9me2) in tumors that were either sensitive or resistant to sunitinib. We performed IHC staining on cut sections of paraffin embedded specimens from the original nephrectomy, the skin metastasis developed on sunitinib, and the derived PDX (RP-R-01), that was again sensitive to sunitinib (12). These tumor samples were obtained from a ccRCC patient who initially responded to sunitinib but then progressed on treatment. Our results showed a significant increase in the expression levels of EZH2 in the skin metastasis as compared to the primary nephrectomy and the derived PDX (Fig. 3A-B). We also observed a parallel increase in the associated histone mark H3K27me3, though not statistically significant. In addition, our result showed differential expression levels of di-methylated H3K4 and H3K9me3 (Supplementary Fig. 5). We detected also increased expression levels of di- and tri-methylated H3K4 and H3K9me3 at the time of resistance to 60 mg/kg sunitinib in the RP-R-01 model (Supplementary Fig. 6). Thus, we wanted to determine whether similar changes occurred in the PDX models RP-R-01 and RP-R-02 following resistance to sunitinib. Interestingly, we observed a transient and reversible increase in the expression levels of EZH2 when tumors became resistant to sunitinib treatment as compared to the sensitive phase, in both PDX models with a return to lower levels with dose escalation to 60 and 80 mg (Fig. 3C). No clear changes in the expression levels of the histone mark H3K27me3 were observed (data not shown). Modulation of EZH2 expression with response or transient resistance to sunitinib was associated with changes in the expression of E-cadherin, a downstream gene product of EZH2 (Fig. 3D). This dynamic inverse correlation of EZH2 and E-cadherin expression levels was also observed in the original set of experiments at the time of sunitinib resistance (Supplementary Fig. 2D).

## Pharmacological and biochemical inhibition of EZH2 in ccRCC cell lines enhances response to sunitinib treatment

To determine to role of EZH2 in modulating the anti-tumor effect of sunitinib we induced either pharmacological or biochemical inhibition of this histone methyltransferase. Mechanistic studies showed that stable transfected cells, 786-0shEZH2_D, have a significant decrease of EZH2 gene/protein expression and an increase in E-cadherin gene expression (Figure 4A and Supplementary Fig. 7A-B). Similar effects were observed by using the EZH2 inhibitor GSK126 (Supplementary Fig. 7A-B). 786-0shEZH2_D cells were more sensitive to sunitinib treatment, as indicated by the significant decrease in cell viability as compared to the scramble control, 786-0shRNA (Fig. 4B). Similarly, we observed a significant decrease in cell viability in 786-0 and 786-0R cells following treatment with the EZH2 inhibitor GSK126 and sunitinib in combination as compared to single agents, with a combination index suggesting synergism (Fig. 4C-D). Interestingly, pharmacological induced reduction in cell viability was associated with reduced expression levels of E2F-1, an upstream target gene of EZH2 (Fig. 4E). The potential role of EZH2 in sunitinib resistance was also suggested by the increased baseline levels of this HMT in the sunitinib resistant cells 786-0R (Fig. 4F).

## Response to sunitinib dose escalation in ccRCC patients

In parallel to the preclinical studies, a subset of ccRCC patients being treated at either the Odette Cancer Centre or Roswell Park Cancer Institute, who initially received sunitinib at

the standard dose and schedule (daily 50 mg, 4 weeks on/2 weeks off) and did not present significant side effects (see Materials and Methods), were offered dose escalation (62.5 mg and 75 mg) at the time of early disease progression (daily dose, 2 weeks on/1 week off). In Fig. 5A and B are depicted the computed tomography (CT) scans of two patients showing the initial progression on 50 mg sunitinib dose and response to 75 mg dose. Table I reports the added progression free survival following the dose escalation.

## DISCUSSION

Acquired resistance to anti-VEGF therapies remains a challenge in the clinical management of patients with ccRCC. Several potential mechanisms that are driving the tumor/host adaptation to this targeted therapeutic strategy have been proposed. In our study, we assessed the effect of sunitinib dose escalation using two TKI sensitive ccRCC PDX models, and showed that the initial drug resistance was transient and reversible. At the time of resistance, as we incrementally increased the sunitinib dose, we observed restored tumor sensitivity to sunitinib in both PDX models. These preclinical observations were mirrored by our clinical experience in a selected group of ccRCC patients who were initially responsive to sunitinib and then became drug resistance. In the absence of significant side effects we were able to increase sunitinib dose from 50 to 62.5 and 75 mg and observed clinical benefit in the majority of the patients. Dose escalation was made feasible by a modified sunitinib schedule of 14 days on and 7 days off that may work better than the standard schedule based on our DCE-US data (20). Our retrospective data suggest that an individualized sunitinib regimen based on this schedule is well tolerated and may induce greater clinical benefit than the traditional schedule (4 weeks on/2 weeks off) likely due to optimal drug exposure for each patient (20). A prospective trial is ongoing in Canadian centers where dose and schedule are individualized based on toxicity and dose escalation is allowed in patients with minimal toxicity on the standard 50 mg dose.

The concept of individualized therapy has multiple examples from the old literature (21). The relationship between exposure to TKIs and efficacy has been previously reported (22, 23) supporting a rationale for sunitinib dose escalation. A large meta-analysis indicated that increased exposure to sunitinib is associated with improved clinical outcomes, though also with some increased risk of adverse effects (23). Despite the clinical use of a universal “flat” dose there are both preclinical and clinical evidences of a dose dependent effect of TKI in RCC. Our tumor growth data in the two PDXs clearly show greater and prolonged effect of high dose sunitinib (80 mg/kg vs 40 mg/kg) with sustained tumor regression in the sunitinib naíve RP-R-02 (Fig. 1A and B). The PK data did not suggest that the transient resistance to sunitinib was due to decreased drug levels. As shown in supplementary Fig. 4, there was a slight increase in plasma concentration of sunitinib in the animal treated with 60 mg/kg as compared to 40 mg/kg, though the difference was not statistically significance. Interestingly, there was a trend for decreased plasma sunitinib concentration following prolonged exposure of the drug, though these differences were not statistically significant. However, we did not observed a significant drop of sunitinib concentrations in the tumors, but rather an increase in the group resistant to 60 mg/kg dose. However, under our experimental conditions we cannot rule out the possibility that PK might have contributed to the reversible tumor sensitivity upon dose escalation of sunitinib, but this looks unlikely, in

view also of the observed intratumor drug accumulation. We can speculate that tumors/host may "adapt" to the pharmacological effects of sunitinib and increased intratumor concentrations, potentially as a consequence of intracellular lysosomal sequestration, may be needed to maintain the same inhibitory effects (11). Previous work has shown that sunitinib may have both anti-angiogenic and anti-cancer effect with the latter perhaps becoming more important at higher doses (11). The assumption that sunitinib may also have a direct anti-tumor effect led us to examine the effect of *in vitro* chronic drug exposure of RCC cells. We used low micromolar sunitinib concentrations that appear to be achievable *in vivo* based on the intra-tumor accumulation reported with this drug (supplementary Fig. 4) (12). We recognize that developing of "resistance" *in vitro* may not necessarily mirror what is happening in patients. However, in our case, *in vitro* chronic exposure of sunitinib induced less sensitivity to sunitinib and it was associated with increased EZH2 expression similarly to what we observed in tumor bearing animals that were exposed to chronic drug administration. Further studies will be necessary to confirm that the *in vitro* biological and molecular changes induced by chronic exposure to sunitinib are predictive of the changes occurring *in vivo*.

The role of TKI dose escalation has been evaluated in a limited set of clinical studies but it remains an unanswered question (24). Intrapatient dose escalation based on drug tolerability has been reported with sorafenib showing clinical benefit but rising also concerns for feasibility due to increased toxicity (25, 26). In a randomized double-blind phase 2 trial, the greater proportion of patients in the axitinib titration group achieved an objective response supporting the rationale for individual drug dose titration with this TKI in selected RCC patients even though this was not associated with a better PFS (27). The potential benefit of escalating the dose of sorafenib at the time of progression has been reported, suggesting that in progressive patients, treatment with a higher dose could be a valid option if tolerated (28). In our limited experience we observed that in 10 out of 16 cases sunitinib dose escalation implemented at the time of disease progression resulted in clinical benefit as shown by a ≥5 month added progression free survival. These preliminary data suggest that intrapatient sunitinib dose escalation at the time of disease progression is feasible in a selected patient population, and may overcome, though transiently in the majority of patients, the initial acquired drug resistance. A prospective clinical study led by Dr. Bjarnason is currently testing this hypothesis in ccRCC patients treated with first-line sunitinib.

Epigenetic modifications have been implicated in cancer progression. Chromatin remodeling gene, have been reported to be altered in RCC (19, 29). Interestingly, over expression of EZH2 has been associated with poorer outcome in patients with RCC (30). In our studies we observed that resistant tumors to sunitinib had an increased level of EZH2 expression. However, this increase was reversible upon dose escalation, suggesting that tumor adaptation to TKI is dynamic, as likely driven by epigenetic alterations. Under our experimental conditions, we observed a correlation between EZH2 expression and H3K27 tri methylation in the original patient tumors but not in the PDX, perhaps due to the already high basal expression of H3K27me3 in the xenografts. Similarly, mechanistic studies suggest that inhibition of EZH2 expression or activity sensitized ccRCC cells to sunitinib *in vitro* and provide a rationale for a potential role of EZH2 in modulating tumor response and

resistance to sunitinib treatment. A downstream target of EZH2 such as E-cadherin was increased with decrease in EZH2 which was also accompanied by a decrease in E2F-1 (31). E2F-1 has been reported in previous studies to play a role in multidrug resistance and negatively regulating cell proliferation when overexpressed (32). In our studies, we also observe increased expression of other histone marks associated with “active” gene expression regulations, such as H3K4me2 and H3K9me2. Further studies will identify the potential genes involved in these epigenetic changes. The current development of EZH2 inhibitors opens the possibility of considering rationale combination strategies with TKI to overcome/delay the initial occurrence of drug resistance. Combining TKIs with other epigenetic therapies, such as histone deacetylase inhibitors and drugs that target hypoxia inducible factors, should also be considered in future clinical trials for ccRCC patients.

In conclusion, our data suggest that sunitinib dose escalation is a potential strategy to reverse initial acquired drug resistance. The molecular mechanism(s) responsible for the tumor resensitization to sunitinib remains to be identified but it seems to be associated with modulation of EZH2 and down-stream target genes. Future studies are warranted to define the role of EZH2 and other epigenetic “drivers” involved in the tumor adaptation and acquired resistance to TKIs.

## Supplementary Material

Refer to Web version on PubMed Central for supplementary material.

## Acknowledgements

We would like to thank the MTMR and Pathology Core Facilities at Roswell Park Cancer Institute for animal handling and processing the tissue samples, respectively. We would like also to acknowledge Jeffery Conroy and Sean Glean at the Genomics Consortium and Genomics Shared Resource at Roswell Park Cancer Institute for helping with the genomic analysis. This research was supported in part by the National Cancer Institute, National Institutes of Health (P30CA016056/1R01CA135321) (RP), a research grant from Pfizer (RP) and a donation from Dr. Richard Turner and Mrs. Deidre Turner (RP).

FINANCIAL INFORMATION: This research was supported in part by the National Cancer Institute, National Institutes of Health (P30CA016056/1R01CA135321) (R. Pili), and a research grant from Pfizer (R.Pili)

Georg Bjarnason and Roberto Pili are paid consultants and has received research funding from Pfizer

## Abbreviations

| | |
|---|---|
| **ccRCC** | clear cell renal cell carcinoma |
| **VEGF** | vascular endothelial growth factor |
| **HMT** | histone methyltransferase |
| **PDX** | patient-derived xenograft |
| **EXH2** | enhancer of zeste homologue 2 |
| **VHL** | Von Hippel Landau |
| **TKI** | tyrosine kinase inhibitors |
| **PRC2** | Polycomb repressive complex 2 |

**bFGF** basic fibroblast growth factor.

## REFERENCES


1. Jemal A, Siegel R, Ward E. Cancer statistics 2013. CA Cancer J Clin. 2013; 63:11–30. [PubMed: 23335087]
2. Pili, R.; Kauffman, E.; Rodriguez, R. Cancer of the Kidney. In: Niederhuber, JE.; Armitage, JO.; Doroshow, JH.; Kastan, MD.; Tepper, JE., editors. Abeloff's Clinical Oncology. Saunders; Philadelphia: 2013. p. 1416-44.
3. Linehan WM, Walter MM, Zbar B. The genetic basis of cancer of the Kidney. J.Urol. 2003; 170:1263–2163.
4. Motzer RJ, Hutson TE, Tomczak P, Michaelson MD, Bukowski RM, Oudard S, et al. Overall survival and updated results for sunitinib compared with interferon alfa in patients with metastatic renal cell carcinoma. J Clin Oncol. 2009; 27:3584–90. [PubMed: 19487381]
5. Lori, Wood. Sunitinib malate for the treatment of renal cell carcinoma. Expert Opin Pharmacother. 2012; 13:1323–36. [PubMed: 22607009]
6. Kerbel RS. Molecular and physiologic mechanisms of drug resistance in cancer: an overview. Cancer Metastasis Rev. 2001; 20:1–2. [PubMed: 11831636]
7. Kerbel RS, Yu J, Tran J, Man S, Viloria-Petit A, Klement G, et al. Possible mechanisms of acquired resistance to anti-angiogenic drugs: implications for the use of combination therapy approaches. Cancer Metastasis Rev. 2001; 20:79–86. [PubMed: 11831651]
8. Ellis LM, Hicklin DJ. VEGF-targeted therapy: mechanisms of anti-tumour activity. Nat Rev Cancer. 2008; 8:579–91. [PubMed: 18596824]
9. Bottsford-Miller JN, Coleman RL, Sood AK. Resistance and escape from antiangiogenesis therapy: clinical implications and future strategies. J Clin Oncol. 2012; 30:4026–34. [PubMed: 23008289]
10. Gerber PA, Hippe A, Buhren BA, Muller A, Homey B. Chemokines in tumor associated angiogenesis. Biol Chem. 2009; 390:1213–1223. [PubMed: 19804363]
11. Gotink KJ, Broxterman HJ, Labots M, de Haas RR, Dekker H, Honeywell RJ, et al. Lysosomal sequestration of sunitinib: a novel mechanism of drug resistance. Clin Cancer Res. 2011; 17:7337–46. [PubMed: 21980135]
12. Hammers HJ, Verheul HM, Salumbides B, Sharma R, Rudek R, Jaspers J, et al. Reversible epithelial to mesenchymal transition and acquired resistance to sunitinib in patients with renal cell carcinoma: evidence from a xenograft study. Mol Cancer Ther. 2010; 9:1525–35. [PubMed: 20501804]
13. Hatziapostolou M, Iliopoulos D. Epigenetic aberrations during oncogenesis. Cell Mol Life Sci. 2011; 68:1681–1702. [PubMed: 21249513]
14. Cao R, Zhang Y. The functions of E(Z)/EZH2-mediated methylation of lysine 27 in histone H3. Curr Opin Genet Dev. 2004; 14:155–164. [PubMed: 15196462]
15. Lu C, Han HD, Mangala LS, Ali-Fehmi R, Newton CS, Ozbun L, et al. Regulation of tumor angiogenesis by EZH2. Cancer Cell. 2010; 32:185–197. [PubMed: 20708159]
16. Li Q, Shi L, Gui B, Yu W, Wang J, Zhang D, et al. Binding of the JmjC demethylase JARID1B to LSD1/NuRD suppresses angiogenesis and metastasis in breast cancer cells by repressing chemokine CCL14. Cancer Res. 2011; 71:6899–908. [PubMed: 21937684]
17. Wagener N, Holland D, Bulkescher J, Crnkovic-Mertens I, Hoppe-Seyler K, Zentgraf H, et al. The enhancer of zeste homolog 2 gene contributes to cell proliferation and apoptosis resistance in renal cell carcinoma cells. Int J Cancer. 2008; 123:1545–50. [PubMed: 18623083]
18. Ougolkov AV, Bilim VN, Billadeau DD. Regulation of pancreatic tumor cell proliferation and chemo resistance by the histone methyltransferase enhancer of zeste homologue 2. Clin Cancer Res. 2008; 14:6790–96. [PubMed: 18980972]
19. Creighton CJ, Morgan M, Gunaratine PH, Wheeler DA, Gibbs RA, Robertson A, et al. Comprehensive molecular characterization of clear cell renal cell carcinoma. Nature. 2013; 499:43–49. [PubMed: 23792563]

20. Bjarnason GA, Khalil B, Hudson JM, Williams R, Milot LM, Atri M, et al. Outcomes in patients with metastatic renal cell cancer treated with individualized sunitinib therapy: Correlation with dynamic microbubble ultrasound data and review of the literature. Urol Oncol. 2014; 32:400–7.
21. Gurney H. Dose calculation of anticancer drugs: a review of the current practice and introduction of an alternative. J Clin Oncol. 1996; 14:2590–611. [PubMed: 8823340]
22. Houk BE, Bello CL, Kang D, Amantea M. A population pharmacokinetic meta-analysis of sunitinib malate (SU11248) and its primary metabolite (SU12662) in healthy volunteers and oncology patients. Clin Cancer Res. 2009; 15:2497–506. [PubMed: 19258444]
23. Houk BE, Bello CL, Poland B, Rosen LS, Demetri GD, Motzer RJ. Relationship between exposure to sunitinib and efficacy and tolerability endpoints in patients with cancer: results of a pharmacokinetic/pharmacodynamic meta-analysis. Cancer Chemother Pharmacol. 2010; 66:357–71. [PubMed: 19967539]
24. Escudier B, Heng DY, Smyth-Medina A, Porta C. Considerations for the design of future clinical trials in metastatic renal cell carcinoma. Clin Genitourin Cancer. 2014; 12:1–12. [PubMed: 24220221]
25. Amato RJ, Harris P, Dalton M, Saxena S, Monzon F, Zhai J, et al. A phase II trial of intra-patient dose-escalated sorafenib in patients (pts) with metastatic renal cell cancer (MRCC). J Clin Oncol. 2008; 15:s5122.
26. Gore ME, Jones RJ, Ravaud A, Kuczyk M, Demkow T, Bearz A, et al. Efficacy and safety of intrapatient dose escalation of sorafenib as first-line treatment for metastatic renal cell carcinoma (mRCC). J Clin Oncol. 2011; 29:s4609.
27. Rini BI, Melichar B, Ueda T, Grünwald V, Fishman MN, Arranz JA, et al. Axitinib with or without dose titration for first-line metastatic renal-cell carcinoma: a randomised double-blind phase 2 trial. Lancet Oncol. 2013; 14:1233–42. [PubMed: 24140184]
28. Mancuso A, Di Paola E, Leone A, Catalano A, Calabro F, Cerbone L, et al. Phase II escalation study of sorafenib in patients with metastatic renal cell carcinoma who have been previously treated with anti-angiogenic treatment. BJU Int. 2012; 109:200–6. [PubMed: 22212284]
29. Varela I, Tarpey P, Raine K, Huang D, Ong CK, Stephens P, et al. Exome sequencing identifies frequent mutation of the SWI/SNF complex gene PBRM1 in renal carcinoma. Nature. 2011; 469:539–42. [PubMed: 21248752]
30. Liu L, Xu Z, Zhong L, Wang H, Jiang S, Long Q, et al. Prognostic value of EZH2 expression and activity in renal cell carcinoma: a prospective study. PLoS One. 2013; 8:e81484. [PubMed: 24312307]
31. Sun NX, Ye C, Zhao Q, Zhang Q, Xu C, Wang SB. Long noncoding RNA-EBIC promotes tumor cell invasion by binding to EZH2 and repressing E-cadherin in cervical cancer. PLoS One. 2014; 9:e100340. [PubMed: 25007342]
32. Yan LH, Wang XT, Yang J, Kong FB, Lian C, Wei WY, et al. Reversal of multidrug resistance in gastric cancer cells by E2F-1 downregulation in vitro and in vivo. J Cell Biochem. 2014; 115:34–41. [PubMed: 24038122]

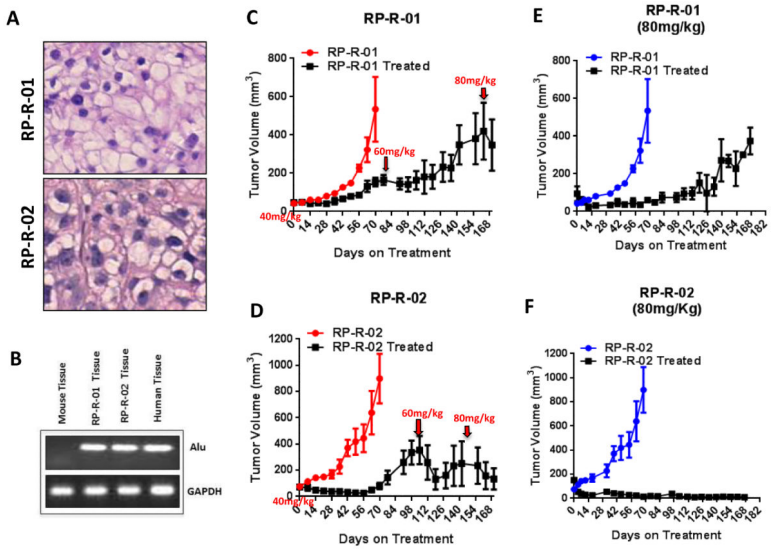


**Figure 1. Tumor growth curve in preclinical ccRCC models in response to sunitinib dose-escalation**

A) H&E staining of tumor samples confirms the original clear cell morphology. B) RNA and DNA were prepared from tumor tissues. Alu expression to determine human origin was assessed by PCR. C-D) Mice bearing RP-R-01 or RP-R-02 tumors were treated with either sunitinib or vehicle. The starting dose of sunitinib was 40 mg/kg daily (5 days/week). Dose was increased to 60 and 80 mg/kg at the time of overt resistance (>50% from nadir). E-F) In a separate experiment, mice bearing RP-R-01 or RP-R-02 tumors were treated with sunitinib 80 mg/kg. Tumor growth was assessed once a week by caliper measurements and body weights by weigh scale. Results are expressed as the mean ± SE.

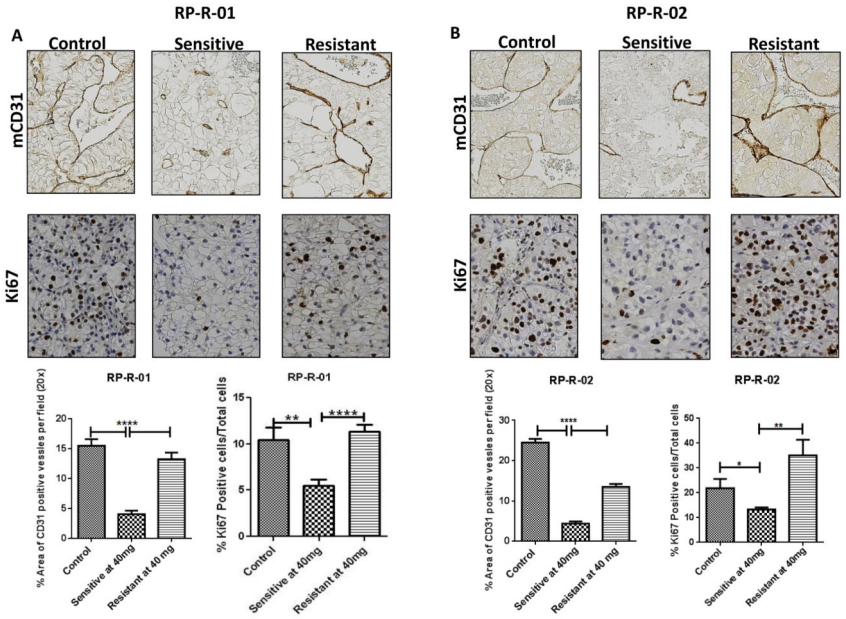


**Figure 2. Immunohistochemical staining for CD31 and Ki67 in RP-R-01 and RP-R-02 tumor**

Tissue samples from RP-R-01 (A) and RP-R-02 (B) were fixed for 24hr, paraffin embedded and cut onto slides. Slides were stained with CD31 and Ki67 antibody. Representative pictures of the immunostaining are depicted (upper panels). Quantitative analyses were performed (lower panels). Results are based on four randomly selected fields per tissue and are expressed as the mean ± SE. Statistical significance was determined by student's t-test. **p<0.01, ***p<0.001.

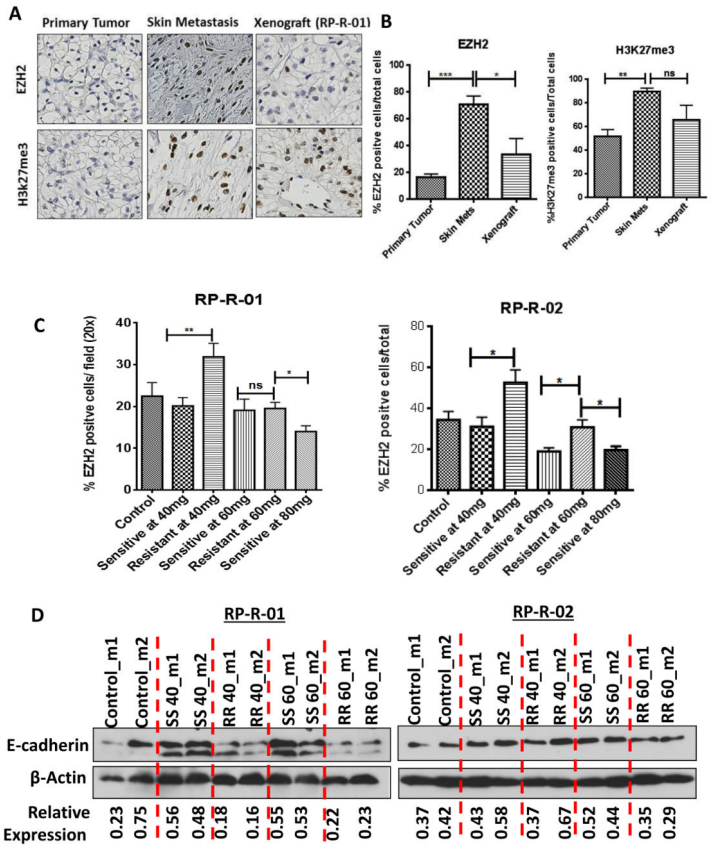


**Figure 3. Epigenetic modification associated with resistance to sunitinib resistance and disease progression**

Sections from the original nephrectomy, the skin metastasis developed on sunitinib from the same patient, and the derived xenograft (RP-R-01) sensitive again to sunitinib were stained for EZH2 and H3K27me3. B) Quantitative analyses were performed. IHC quantitative results are based on four randomly selected fields per tissue and are expressed as the mean % positive cells/total cells ± SE. C) As shown in Fig. 1A-B, tissue samples from control, tumors sensitive and resistant to sunitinib at each dose were fixed for 24hr and paraffin embedded. Quantitative analyses were performed. D) Expression levels of E-cadherin were assessed by immunoblotting assay of tumor lysates. Total β-actin was also assessed as loading control and relative expression levels were determined by densitometry. Statistical significance was determined by student's t-test. *p<0.05, **p<0.01, ***p< 0.001 ns= not significant.

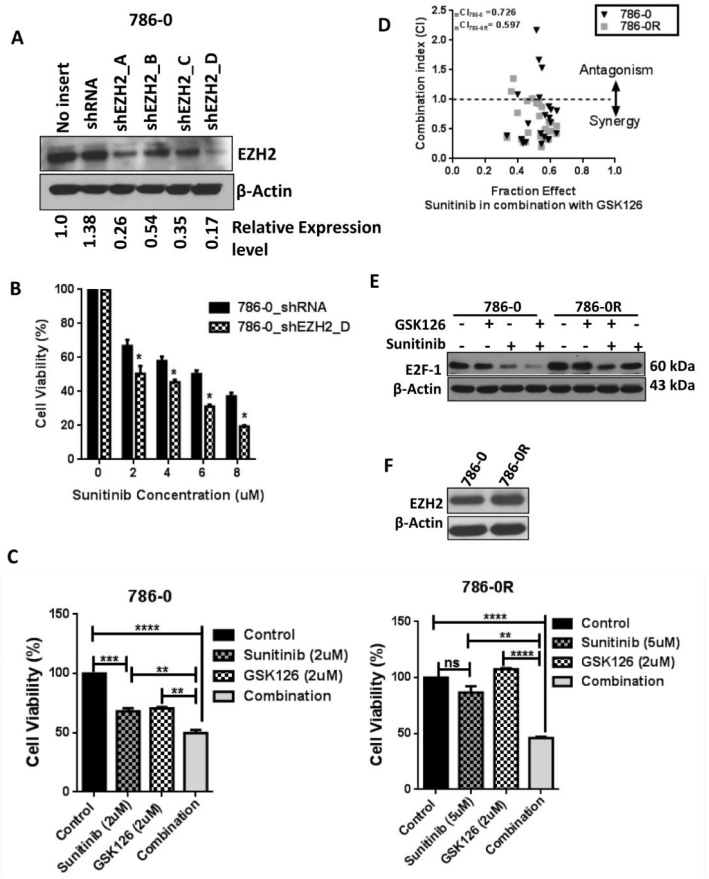


**Figure 4. Increased sensitivity to sunitinib following biochemical and pharmacological inhibition of EZH2 in ccRCC cell lines**

A) Western blot analysis showing the efficiency of EZH2 knockdown in 786-0 cell line. B) Specific knockdown of EZH2 in 786-0 cells are more sensitive to sunitinib as compare to the scrambled template control, 786-0_shRNA. C) 786-0 and 786-0R cell lines were treated with either sunitinib, GSK126 or both for 48hr. Bar chart indicates significant decrease in cell viability in combination treatment arm as compared to the single agents alone. D) Combination index values for sunitinib and GSK126 in 786-0 (CI=0.224) and 786-0R (CI=0.224). E) Western blot analysis shows a decrease in E2F-1 with single treatments or combination in 786-0 cells however, in the resistant cell lines, expression levels are significantly low in combination treatment. F) Western blot analysis showing increase in EZH2 expression in sunitinib resistant cell lines, 786-0R compared to the parental 786-0.

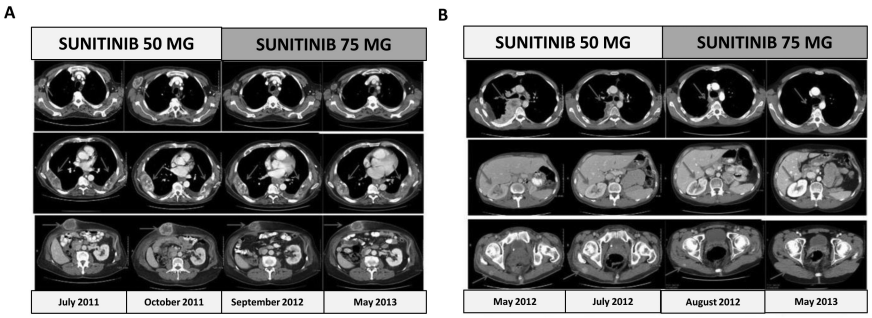


**Figure 5. Response to sunitinib dose-escalation in patients with clear cell renal cell carcinoma**

Two patients with ccRCC who were initially responsive to 50 mg of sunitinib eventually became resistance. Increased dose of 75mg restored response to sunitinib. A) and B) representative CT images from two patients and arrows indicate tumor lesions.

**Table I**

Clinical benefit in patients with sunitinib dose-escalation

| SUNITINIB DOSE ESCALATION FROM 50 MG DOSE | ADDED PFS AFTER DOSE ESCALATION |
|---|---|
| 62.5 mg | 11 months |
| 62.5 mg | 10 months |
| 62.5 mg | 8 months |
| 62.5 mg | 16 months & currently ongoing |
| 62.5 mg | 6 months |
| 62.5 mg | 5 months |
| 75 mg | 15 months |
| 62.5 mg | 3 months |
| 75 mg | 3 weeks |
| 62.5 mg | 2 months |
| 62.5 mg | 2 months |
| 62.5 mg | 5 months |
| 62.5 mg | 2 months |
| 75 mg | 5 months |
| 62.5 mg | 1 months |
| 75 mg | 17 months & currently ongoing |
| 75 mg | 24 months & currently ongoing |
| 75 mg | 21 months |
| 75 mg | 4 months |
| 75 mg | 2 months |